

## Spin Depolarization due to Beam-Beam Interaction in NLC\*

Kathleen A. Thompson  
Stanford Linear Accelerator Center, Stanford University, Stanford, CA 94309

### Abstract

Calculations of spin depolarization effects due to the beam-beam interaction are presented for several NLC designs. The depolarization comes from both classical (Bargmann-Michel-Telegdi precession) and quantum (Sokolov-Ternov spin-flip) effects. It is anticipated that some physics experiments at future colliders will require a knowledge of the polarization to better than 0.5% precision. We compare the results of CAIN simulations with the analytic estimates of Yokoya and Chen for head-on collisions.<sup>†</sup> We also study the effects of transverse offsets and beamstrahlung-induced energy spread.

<sup>†</sup> K.Yokoya and P.Chen, 8th International Conference on High Energy Spin Physics, Minneapolis, 12-17 September 1988.

*Presented at Advanced ICFA Beam Dynamics Workshop on Quantum Aspects  
of Beam Physics, Capri, Italy, October 10-15, 2000*

---

\*Work supported by Department of Energy contract DE-AC03-76SF00515.

# SPIN DEPOLARIZATION DUE TO BEAM-BEAM INTERACTION IN NLC

KATHLEEN A. THOMPSON  
*Stanford Linear Accelerator Center*  
*Stanford University, Stanford, CA 94309*  
*E-mail: kthom@SLAC.Stanford.edu*

Calculations of spin depolarization effects due to the beam-beam interaction are presented for several NLC designs. The depolarization comes from both classical (Bargmann-Michel-Telegdi precession) and quantum (Sokolov-Ternov spin-flip) effects. It is anticipated that some physics experiments at future colliders will require a knowledge of the polarization to better than 0.5% precision. We compare the results of CAIN simulations with the analytic estimates of Yokoya and Chen for head-on collisions.<sup>1</sup> We also study the effects of transverse offsets and beamstrahlung-induced energy spread.

## 1 Introduction

In this note we give simulation and analytic results for the depolarization due to the beam-beam interaction in NLC nominal designs and some high-luminosity variations. Such depolarization effects are negligibly small in the SLC. However for precision tests of the Standard Model in NLC, it will be necessary to know the beam polarization to within a few tenths of a percent, which is comparable to the amount of luminosity-averaged depolarization due to the beam-beam interaction in NLC. Furthermore, the beam disruption is higher in NLC than in SLC, which makes it more difficult to obtain accurate measurements of the final polarization using a Compton polarimeter in the extraction line; hence accurate calculations of the beam-beam depolarization are needed.

We used the program CAIN<sup>2</sup> to simulate the beam-beam collisions. At present, CAIN is the only beam-beam simulation program that calculates depolarization effects. Application of CAIN for some NLC depolarization calculations has been previously reported on by Weidemann.<sup>3</sup> One purpose of our paper is to compare simulation results with analytic estimates<sup>1</sup> for a variety of NLC parameter sets and thus help validate the code.

The strength of the beam-beam interaction may be characterized by

$$\Upsilon \equiv \frac{e\hbar}{m^3c^4} \sqrt{|F_{\mu\nu}p^\nu|^2} = \gamma \frac{E+B}{F_c} \quad , \quad (1)$$

where  $p^\nu = (E, \vec{p})$  is the 4-momentum of the incoming electrons or positrons,  $m$  is the electron mass,  $\gamma \equiv E/mc^2$  is the Lorentz factor,  $F_{\mu\nu}$  is the energy-momentum tensor of the electromagnetic field produced by the oncoming beam,

and  $F_c \equiv m^2 c^3 / \hbar e \approx 4.4 \times 10^{13}$  Gauss is the Schwinger critical field. Sometimes the parameter  $\xi$  is used instead:

$$\xi \equiv \frac{u_c}{m\gamma} \quad . \quad (2)$$

Here  $u_c$  is the critical energy of the classical synchrotron radiation spectrum.  $\Upsilon$  and  $\xi$  are relativistic invariants and are related by  $\Upsilon = \frac{3}{2}\xi$ . For small disruption and gaussian beams, the effective value of  $\Upsilon$  is given by<sup>4</sup>

$$\Upsilon_{eff} = \frac{5Nr_e^2\gamma}{6\alpha\sigma_z(\sigma_x + \sigma_y)} \quad , \quad (3)$$

where  $N$  is the number of particles per bunch,  $r_e$  is the classical electron radius,  $\alpha$  is the fine-structure constant,  $\sigma_{x,y}$  are the transverse bunch sizes, and  $\sigma_z$  is the bunch length.

## 2 Analytic estimates for beam-beam depolarization

There are two significant mechanisms of beam-beam depolarization. One, the BMT effect, arises from the classical precession of the longitudinally-polarized electrons in the beam-beam field, in accordance with the Bargmann-Michel-Telegdi equation. The other, Sokolov-Ternov spin-flip (ST effect), tends to polarize electrons along the magnetic field ( $e^+$  parallel,  $e^-$  anti-parallel) and thus degrades the longitudinal polarization since the magnetic field is perpendicular to the longitudinal axis. Analytic estimates for both these effects have been previously derived by Yokoya and Chen.<sup>1</sup>

Following Yokoya and Chen (YC), the final outgoing depolarization will be denoted by angle brackets, i.e.  $\langle \Delta P \rangle$ , and the luminosity-weighted depolarization by square brackets, i.e.  $[\Delta P]$ . According to YC,  $\langle \Delta P \rangle$  and  $[\Delta P]$  are related by

$$[\Delta P] \approx 0.273 \langle \Delta P \rangle \quad . \quad (4)$$

This is valid for both the BMT and ST contributions provided that the horizontal disruption  $D_x \ll 1$ .

YC's estimate of the depolarization due to the BMT effect is

$$\langle \Delta P_{BMT} \rangle \approx \frac{3}{50\pi^2} n_{cl}^2 \left[ \frac{a(\Upsilon_{eff})}{a(0)} \right]^2 \approx 0.0061 n_{cl}^2 \left[ \frac{a(\Upsilon_{eff})}{a(0)} \right]^2 \quad . \quad (5)$$

The factor in square brackets was calculated by V.Baier<sup>5</sup> (see the CAIN manual<sup>2</sup>) and  $n_{cl}$  is the average number of synchrotron photons emitted per electron according to classical synchrotron radiation theory, which is given in YC

as:

$$n_{cl} = \frac{5\sqrt{\pi}}{2\sqrt{3}}(\sqrt{2} - 1) \frac{\alpha r_e N}{\sqrt{\sigma_x \sigma_y}} f(R) \quad , \quad (6)$$

where  $R = \sigma_x/\sigma_y$  and  $f(R) \equiv \frac{2\sqrt{R}}{1+R}$ .

YC's estimate of the depolarization due to the ST effect is

$$\langle \Delta P_{ST} \rangle \approx 2U_f(\xi_{eff})n_{cl} = 2\frac{U_f(\xi_{eff})}{U_0(\xi_{eff})}n_\gamma \quad , \quad (7)$$

which is always less than  $0.04n_\gamma$ .  $U_f(\xi)$  and  $U_0(\xi)$  may be expressed in terms of modified Bessel functions; formulas for and plots of these functions are given by YC.<sup>1</sup> Note that the actual number of synchrotron photons emitted per electron is given by  $n_\gamma = U_0(\xi)n_{cl}$ .

### 3 Basic parameters for six baseline designs and variations

We give some luminosity-related parameters for the basic NLC designs<sup>6</sup> near 0.5, 1.0, and 1.5 TeV center of mass energy in Tables 1, 2, and 3. The quantities  $\mathcal{L}_D$  and  $\mathcal{L}_D$  are the luminosity per bunch (in units  $\text{m}^{-2}$ ), with and without the pinch enhancement due to disruption. The quantity  $L_D$  is the luminosity (in units  $\text{cm}^{-2}\text{sec}^{-1}$ ) taking into account the repetition rate and number of bunches per train.

Parameters for some alternative designs that are also under consideration for NLC are given in Table 4. These are designs which have equal beta functions in the horizontal and vertical directions, and thus the beams are less flat. This leads to significantly higher disruption and beamstrahlung, as well as higher depolarization.

### 4 Polarization Results

In Table 5 we give the final outgoing depolarization for the nominal NLC designs. For comparison we show the results from the analytic formulas discussed above, as well as the results from CAIN simulations. The ST depolarization in CAIN simulations can only be done if BMT depolarization is also turned on, so the simulation result quoted for ST alone,  $\langle \Delta P_{ST} \rangle$ , is simply the difference  $\langle \Delta P_{tot} \rangle - \langle \Delta P_{BMT} \rangle$ , where  $\langle \Delta P_{BMT} \rangle$  is the result with only BMT turned on, and  $\langle \Delta P_{tot} \rangle$  is the result with both BMT and ST turned on. In Table 6 we give the luminosity-weighted outgoing depolarization for the nominal NLC designs, again including the results from both the analytic formulas and CAIN simulations. The analytic results are somewhat higher than the simulation results for the BMT case; it is expected that the

Table 1: IP parameters for three  $\sim 1/2$  TeV c.m. NLC designs

|   | A-500      | B-500     | C-500      |
|---|------------|-----------|------------|
| $E_{beam}$ [GeV]  | 267.5      | 257.5     | 250.       |
| N [ $10^{10}$ ]   | 0.75       | 0.95      | 1.1        |
| $\gamma\epsilon_x/\gamma\epsilon_y$ [ $\mu\text{m-r}$ ] | 4.0/0.06   | 4.5/0.1   | 5.0/0.14   |
| $\beta_x/\beta_y$ [mm]                                  | 10/0.1     | 12/0.12   | 13/0.2     |
| $\sigma_z$ [ $\mu\text{m}$ ]                            | 90.        | 120.      | 145.       |
| $\sigma_x/\sigma_y$ [nm]                                | 276/3.4    | 327/4.9   | 365/7.6    |
| $\mathcal{L}_0$ [ $10^{33} \text{ m}^{-2}$ ]            | 4.78       | 4.50      | 3.50       |
| $A_x/A_y$   | 0.009/0.90 | 0.010/1.0 | 0.011/0.73 |
| $D_x/D_y$   | 0.094/7.7  | 0.117/7.9 | 0.136/6.5  |
| $\Upsilon_{eff}$  | 0.14       | 0.11      | 0.09       |
| $\mathcal{L}_D$ [ $10^{33} \text{ m}^{-2}$ ]            | 6.51       | 5.84      | 5.21       |
| $H_D$   | 1.36       | 1.30      | 1.49       |
| $n_\gamma$  | 1.08       | 1.18      | 1.24       |
| $\delta_B$  | 4.3%       | 3.9%      | 3.7%       |
| Bunches/train   | 95         | 95        | 95         |
| Rep. rate   | 120        | 120       | 120        |
| $L_D$ [ $10^{33} \text{ cm}^{-2} \text{ sec}^{-1}$ ]    | 7.42       | 6.66      | 5.94       |

Table 2: IP parameters for three  $\sim 1$  TeV c.m. NLC designs

|   | A-1000     | B-1000    | C-1000      |
|---|------------|-----------|-------------|
| $E_{beam}$ [GeV]  | 523.       | 504.      | 489.        |
| N [ $10^{10}$ ]   | 0.75       | 0.95      | 1.1         |
| $\gamma\epsilon_x/\gamma\epsilon_y$ [ $\mu\text{m-r}$ ] | 4.0/0.06   | 4.5/0.1   | 5.0/0.14    |
| $\beta_x/\beta_y$ [mm]                                  | 10/0.125   | 12/0.15   | 13/0.2      |
| $\sigma_z$ [ $\mu\text{m}$ ]                            | 90.        | 120.      | 145.        |
| $\sigma_x/\sigma_y$ [nm]                                | 198/2.7    | 234/3.9   | 261/5.4     |
| $\mathcal{L}_0$ [ $10^{33} \text{ m}^{-2}$ ]            | 8.37       | 7.87      | 6.83        |
| $A_x/A_y$   | 0.009/0.72 | 0.01/0.80 | 0.011/0.725 |
| $D_x/D_y$   | 0.094/6.9  | 0.103/7.0 | 0.136/6.5   |
| $\Upsilon_{eff}$  | 0.39       | 0.30      | 0.25        |
| $\mathcal{L}_D$ [ $10^{33} \text{ m}^{-2}$ ]            | 12.4       | 11.4      | 10.2        |
| $H_D$   | 1.50       | 1.44      | 1.50        |
| $n_\gamma$  | 1.4        | 1.5       | 1.6         |
| $\delta_B$  | 9.5%       | 9.2%      | 8.7%        |
| Bunches/train   | 95         | 95        | 95          |
| Rep. rate   | 120        | 120       | 120         |
| $L_D$ [ $10^{33} \text{ cm}^{-2} \text{ sec}^{-1}$ ]    | 14.3       | 12.9      | 11.7        |

Table 3: IP parameters for two  $\sim 1.5$  TeV c.m. NLC designs

|   | A-1500     | B-1500     |
|---|------------|------------|
| $E_{beam}$ [GeV]  | 703        | 739        |
| N [ $10^{10}$ ]   | 1.4        | 0.95       |
| $\gamma\epsilon_x/\gamma\epsilon_y$ [ $\mu\text{m-r}$ ] | 4.5/0.14   | 4.5/0.1    |
| $\beta_x/\beta_y$ [mm]                                  | 15/0.2     | 13/0.2     |
| $\sigma_z$ [ $\mu\text{m}$ ]                            | 130.       | 150.       |
| $\sigma_x/\sigma_y$ [nm]                                | 222/4.5    | 201/3.7    |
| $\mathcal{L}_0$ [ $10^{33} \text{ m}^{-2}$ ]            | 15.6       | 9.6        |
| $A_x/A_y$   | 0.009/0.65 | 0.012/0.75 |
| $D_x/D_y$   | 0.15/7.3   | 0.14/7.3   |
| $\Upsilon_{eff}$  | 0.60       | 0.41       |
| $\mathcal{L}_D$ [ $10^{33} \text{ m}^{-2}$ ]            | 25.1       | 14.4       |
| $H_D$   | 1.61       | 1.50       |
| $n_\gamma$  | 2.2        | 1.7        |
| $\delta_B$  | 17%        | 12%        |
| Bunches/train   | 95         | 95         |
| Rep. rate   | 60         | 90         |
| $L_D$ [ $10^{33} \text{ cm}^{-2} \text{ sec}^{-1}$ ]    | 14.3       | 12.3       |

analytic BMT result may be an overestimate since it does not take account of the fact that the polarization vector will oscillate back and forth across the longitudinal axis when the disruption is high. Apart from this, the agreement between analytic and simulation results is quite good (of course this does not prove that they agree with nature, but does give some degree of confidence).

In Table 7 we give the final outgoing depolarization and in Table 8 the luminosity-weighted depolarization, for the two designs shown in Table 4. These have significantly higher depolarization than the nominal designs. Since the beam-beam disruption and consequent pinching of the beam are much higher in this case, a better analytic approximation can be obtained by taking the modification of the effective transverse beam size into account according to a prescription given by Chen<sup>7</sup>. This beam size correction to the analytic estimate is negligible for the NLC nominal designs, but is significant for the higher luminosity designs. Including the correction brings the analytic and simulation results into good agreement for the EqBetas1 case, but there is still some discrepancy for the EqBetas2 case, which has the highest depolarization.

Since there is always some jitter in the beam position at the IP, it is also of interest to look at the depolarization as a function of the offset of the two beams. CAIN simulation results for depolarization versus horizontal and

Table 4: IP parameters for two modified  $\sim 1.0$  TeV c.m. NLC designs, with equal beta functions

|   | EqBetas1    | EqBetas2    |
|---|-------------|-------------|
| $E_{beam}$ [GeV]  | 504         | 504         |
| N [ $10^{10}$ ]   | 0.475       | 0.55        |
| $\gamma\epsilon_x/\gamma\epsilon_y$ [ $\mu\text{m-r}$ ] | 4.5/0.1     | 4.5/0.1     |
| $\beta_x/\beta_y$ [mm]                                  | 1.3/1.3     | 1.3/1.3     |
| $\sigma_z$ [ $\mu\text{m}$ ]                            | 120.        | 120.        |
| $\sigma_x/\sigma_y$ [nm]                                | 77/11.5     | 77/11.5     |
| $\mathcal{L}_0$ [ $10^{33} \text{ m}^{-2}$ ]            | 2.03        | 2.72        |
| $A_x/A_y$   | 0.092/0.092 | 0.092/0.092 |
| $D_x/D_y$   | 0.48/3.2    | 0.56/3.7    |
| $\Upsilon_{eff}$  | 0.50        | 0.62        |
| $\mathcal{L}_D$ [ $10^{33} \text{ m}^{-2}$ ]            | 4.68        | 6.81        |
| $H_D$   | 2.3         | 2.5         |
| $n_\gamma$  | 2.2         | 2.7         |
| $\delta_B$  | 16%         | 20%         |
| Bunches/train   | 190         | 190         |
| Rep. rate   | 120         | 120         |
| $L_D$ [ $10^{33} \text{ cm}^{-2} \text{ sec}^{-1}$ ]    | 10.7        | 15.5        |

vertical offsets, for the NLC-B-1000 design, are shown in Figure 1. In this figure, plots for horizontal offsets are on the left and vertical offsets on the right. The two plots on the top show the outgoing depolarization, the middle plots show the luminosity-weighted depolarization, and the bottom plots show the ratio of the luminosity-weighted to the outgoing depolarization. Total depolarization is shown as a solid curve and BMT-only depolarization as a dashed curve. The difference between total and BMT-only (representing ST depolarization) is shown as a dotted curve. Only the vertical offset gives a noticeable effect on the luminosity-weighted depolarization, and even here it is quite small – only 0.2% for a  $\Delta y = 2\sigma_y$  offset.

The depolarization as function of beamstrahlung-induced energy spread is illustrated by Figure 2, which shows the correlation between energy and depolarization of the macroparticles in an NLC-B-1000 simulation. Figure 3 shows histograms of the average depolarization (top) and number of electron beam macroparticles (bottom), as a function of macroparticle energy. This dependence of depolarization on energy of individual beam particles is a very significant effect that would need to be taken into account in studies of processes whose cross sections peak significantly below the nominal CM energy.

In conclusion, the simulation results agree well with the analytic estimates when the depolarization is not more than a few percent. We assume that the disagreements seen at larger depolarizations are due to the assumptions in the analytic approximations not being as well satisfied.

I thank K. Yokoya, M. Woods, and P.Chen for helpful discussions related to this work.

Table 5: Final outgoing electron beam depolarization  $\langle \Delta P \rangle$ , for nominal NLC designs. "anlyt" denotes analytic results, "sim" denotes CAIN simulation results.

|            | BMT   | ST    | TOTAL | BMT  | ST     | TOTAL |
|------------|-------|-------|-------|------|--------|-------|
|            | anlyt | anlyt | anlyt | sim  | sim    | sim   |
| NLC-A-500  | 0.6%  | 0.4%  | 1.1%  | 0.4% | (0.5%) | 0.9%  |
| NLC-B-500  | 0.8%  | 0.4%  | 1.1%  | 0.5% | (0.4%) | 0.9%  |
| NLC-C-500  | 0.9%  | 0.3%  | 1.1%  | 0.5% | (0.3%) | 0.9%  |
| NLC-A-1000 | 0.8%  | 2.0%  | 2.8%  | 0.5% | (1.6%) | 2.1%  |
| NLC-B-1000 | 1.0%  | 1.4%  | 2.5%  | 0.6% | (1.3%) | 2.0%  |
| NLC-C-1000 | 1.2%  | 1.2%  | 2.4%  | 0.8% | (1.2%) | 1.9%  |
| NLC-A-1500 | 1.6%  | 3.8%  | 5.4%  | 1.1% | (3.4%) | 4.5%  |
| NLC-B-1500 | 1.2%  | 2.1%  | 3.2%  | 0.7% | (2.0%) | 2.7%  |

Table 6: Luminosity-weighted electron beam depolarization  $[\Delta P]$ , for nominal NLC designs

|            | BMT   | ST    | TOTAL | BMT  | ST     | TOTAL |
|------------|-------|-------|-------|------|--------|-------|
|            | anlyt | anlyt | anlyt | sim  | sim    | sim   |
| NLC-A-500  | 0.2%  | 0.1%  | 0.3%  | 0.1% | (0.1%) | 0.2%  |
| NLC-B-500  | 0.2%  | 0.1%  | 0.3%  | 0.1% | (0.1%) | 0.2%  |
| NLC-C-500  | 0.2%  | 0.1%  | 0.3%  | 0.1% | (0.1%) | 0.2%  |
| NLC-A-1000 | 0.2%  | 0.5%  | 0.8%  | 0.1% | (0.4%) | 0.5%  |
| NLC-B-1000 | 0.3%  | 0.4%  | 0.7%  | 0.1% | (0.3%) | 0.5%  |
| NLC-C-1000 | 0.3%  | 0.3%  | 0.7%  | 0.2% | (0.3%) | 0.4%  |
| NLC-A-1500 | 0.4%  | 1.0%  | 1.5%  | 0.2% | (0.9%) | 1.1%  |
| NLC-B-1500 | 0.3%  | 0.6%  | 0.9%  | 0.1% | (0.5%) | 0.6%  |

## References

1. K.Yokoya and P.Chen, 8th International Conference on High Energy Spin Physics, Minneapolis, 12-17 September 1988; SLAC-PUB-4692.
2. K.Yokoya, "User's Manual of CAIN", 1997.
3. Achim W.Weidemann, Int.J.Mod.Physics A, 2537 (2000).
4. K.Yokoya and P.Chen, in M.Dienes, et.al. (ed.), Frontiers of Particle Beams: Intensity Limitations (Springer-Verlag, 1988).
5. V.Baier, unpublished.
6. NLC parameters as of 1998.
7. P.Chen, Particle Accelerator Conference, Washington, DC, 17-20 May, 1993

Table 7: Final outgoing electron beam depolarization  $\langle \Delta P \rangle$ , for two equal-beta NLC designs. Starred values are analytic estimates with reduction of transverse beam size due to disruption taken into account.

|          | BMT<br>anlyt   | ST<br>anlyt     | TOTAL<br>anlyt   | BMT<br>sim | ST<br>sim | TOTAL<br>sim |
|----------|----------------|-----------------|------------------|------------|-----------|--------------|
| EqBetas1 | 2.0%<br>1.6% * | 3.1%<br>3.8% *  | 5.1%<br>5.4% *   | 1.6%       | (3.7%)    | 5.3%         |
| EqBetas2 | 3.7%<br>1.7% * | 7.8%<br>10.3% * | 11.5%<br>12.0% * | 2.5%       | (9.8%)    | 12.4%        |

Table 8: Luminosity-weighted electron beam depolarization  $[\Delta P]$ , for two equal-beta NLC designs. Starred values are analytic estimates with reduction of transverse beam size due to disruption taken into account.

|          | BMT<br>anlyt   | ST<br>anlyt    | TOTAL<br>anlyt | BMT<br>sim | ST<br>sim | TOTAL<br>sim |
|----------|----------------|----------------|----------------|------------|-----------|--------------|
| EqBetas1 | 0.6%<br>0.4% * | 0.9%<br>1.0% * | 1.4%<br>1.5% * | 0.4%       | (1.1%)    | 1.5%         |
| EqBetas2 | 1.0%<br>0.5% * | 2.1%<br>2.8% * | 3.2%<br>3.3% * | 0.7%       | (3.4%)    | 4.2%         |

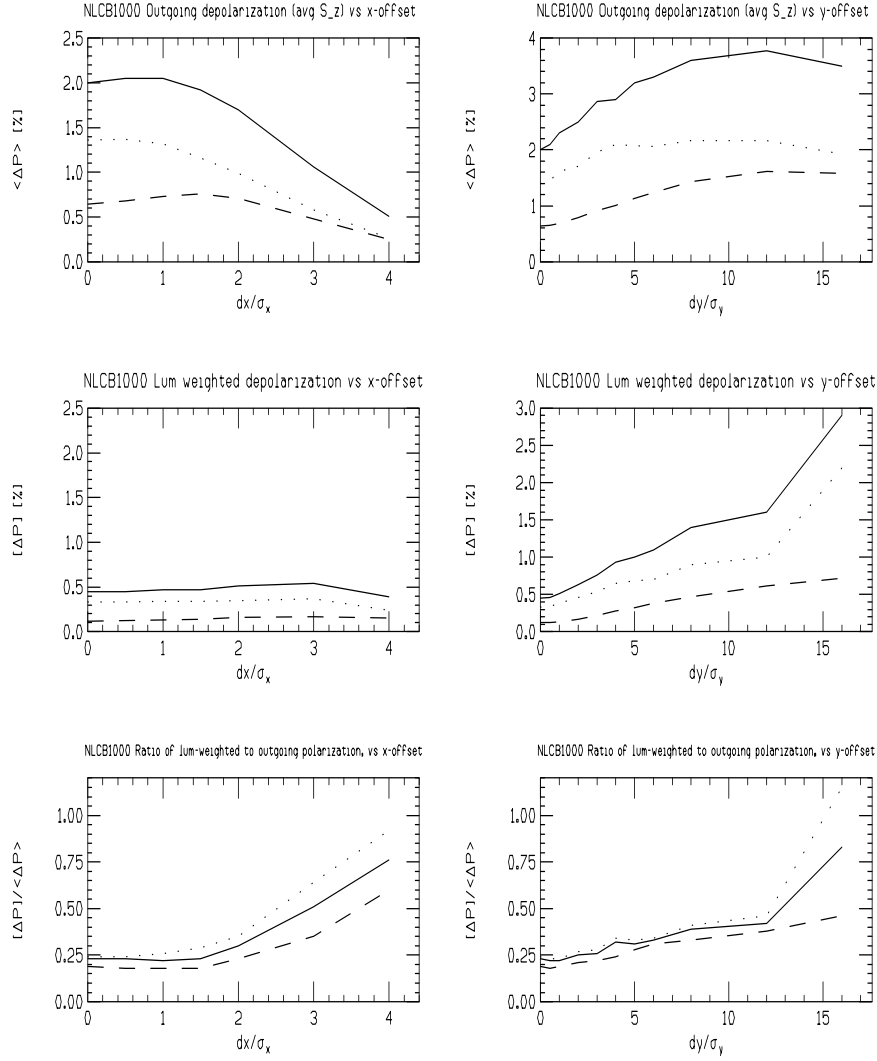


Figure 1: Top: Final outgoing polarization, Middle: Luminosity-weighted polarization, Bottom: Ratio of luminosity-weighted polarization to final outgoing polarization, as a function of horizontal (figures on left) and vertical offset (figures on right) for NLC-B-1000 design. Total depolarization (solid curve), BMT-only depolarization (dashed curve), Difference between total and BMT-only representing ST depolarization (dotted curve).

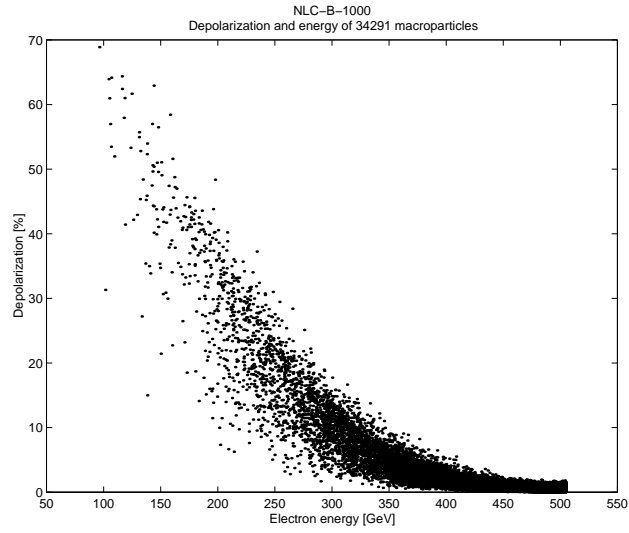


Figure 2: Depolarization and energy of 34291 electron beam macroparticles, for NLC-B-1000 design.

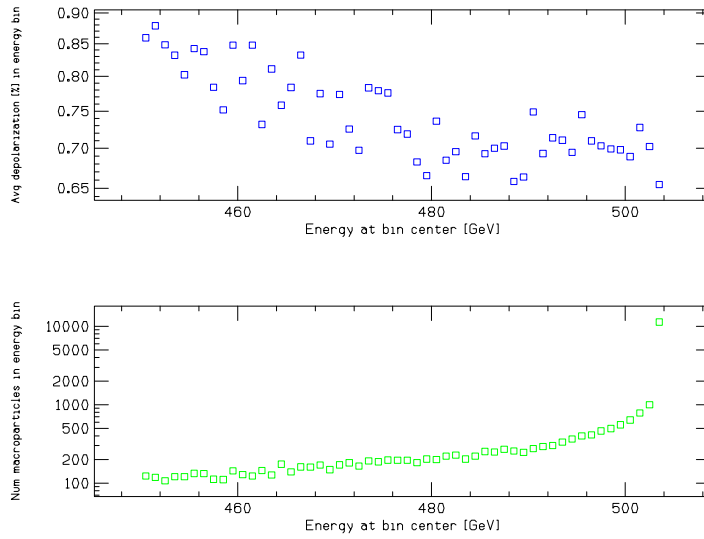


Figure 3: Histograms of average depolarization (top) and number of electron beam macroparticles (bottom), as a function of macroparticle energy, for NLC-B-1000 design.